



Introducing Padded Wall to Reduce Sloshing Induced Wall Pressure in Water Storage Tanks

R. Mahmoudi, F. Ashrafzadeh, S. Tariverdilo*

Department of Civil Engineering, University of Urmia, Urmia, Iran

PAPER INFO

Paper history:

Received 13 February 2014

Received in revised form 01 August 2014

Accepted 14 August 2014

Keywords:

Sloshing

Velocity Potential Function

Padded Wall

Water Storage Tank

ABSTRACT

Sloshing due to ground motion develops large pressure on the walls of water retaining tanks. This paper evaluates the efficacy of padded walls on the reduction of sloshing effects in rectangular water storage tanks subjected to ground motion. An analytical solution based on velocity potential function is provided to obtain the response of rigid and padded wall tanks in terms of wave elevation, maximum pressure on the tank wall and FFT spectrum of pressure on the water surface. In the proposed method, the boundary condition on the tank wall is kinetic representing pressure distribution on the tank walls against the usual methods with kinematic boundary condition only. The fluid is assumed to be inviscid, incompressible, and irrotational. Tanks with and without padded walls are evaluated under different types of ground motions classified as near source and far-field records. The results show noteworthy effect of the padded wall on reduction of above-mentioned sloshing responses.

doi: 10.5829/idosi.ije.2014.27.12c.04

1. INTRODUCTION

Partially filled liquid storage tanks subjected to ground motion may be damaged under fluid fluctuation. This phenomenon is known as sloshing. Sloshing imposing large pressure on the tank wall could cause severe structural damages. Violent oscillation due to sloshing could occur in tanks with natural frequencies close to the excitation frequency.

Many researchers have paid attention to sloshing response of liquid storage tanks. Abramson [1] studied sloshing in partially filled tanks. He used velocity potential function to evaluate the response of cylindrical tanks. Hwang et al. [2] used numerical and experimental methods to investigate sloshing in two and three-dimensional liquid containers. They found good agreement between the results of the two methods. Virella et al. [3] studied sloshing modes and pressure in rectangular tanks under harmonic excitation. They used linear wave theory (LWT) and nonlinear wave theory (NLWT) in ABAQUS software. Wang and Khoo [4]

employed finite element method (FEM) to study response parameters such as wave height and wall pressure in 2D tanks under random excitation. Tariverdilo et al. [5] investigated the importance of membrane and flexural stress in floating roofs of cylindrical liquid storage tanks. Shabani [6] studied the stress pattern in single deck floating roof with pontoon. Azhdari Moghaddam [7] investigated the design issues of surge tanks.

Many researchers used different forms of baffles as sloshing suppression device. Isaacson and Premasiri [8] investigated damping in tanks with baffles as they cause flow separation and increase inherent material damping. Experimental studies were conducted on the rectangular tanks of various filling depth and different rolling frequencies with and without ring baffles by Akyildiz et al. [9]. Results demonstrated that the arrangement of baffles is effective in sloshing reduction. On the other hand, Cho and Lee [10] applied velocity potential based nonlinear FEM to investigate the effect of baffle height and width in two-dimensional rectangular tanks. Panigrahy et al. [11] conducted experimental studies on rectangular tanks with and without baffles. They used shaking table to excite a square tank with different

*Corresponding Author's Email: s.tariverdilo@urmia.ac.ir (S. Tariverdilo)

frequencies and filling levels. Jung et al. [12] studied the effect of vertical baffle height on sloshing reduction in moving 3D rectangular tank. Pal and Bhattacharyya [13] applied finite element method to study sloshing effect on cylindrical tank wall in rigid and flexible cases. Koller and Malhotra [14] studied the effect of slenderness ratio and variety of liquids in cylindrical tanks. Accordingly, fundamental natural frequency lengthening is proposed to reduce sloshing effects. Liu and Lin [15] employed numerical method to study 3D sloshing in tank with baffles. The effect of vertical baffles on pressure and free surface displacement reduction was taken into account. Results showed the effective performance of baffles. Belakroum et al. [16] applied a passive technique to reduce sloshing. To study the effect of baffle in different sizes and locations in rectangular tanks, finite element method known as Galerkin Last Square (GLS) is applied. Maleki and Ziyaeifar [17] studied the damping effect of horizontal ring and vertical blade baffle in cylindrical tanks under horizontal excitation analytically. Also, experimental studies were conducted on the shake table to validate the analytical results.

The main interest in employing baffles is reduction in sloshing height, while the force exerted on tank walls even could be increased. On the other hand, in seismic retrofit of tanks, the common way is to strengthen tank by increasing its stiffness and strength. However, another option could be reducing seismic force demand on tank walls to avoid expansive and timely methods based on strengthening of the tank.

Accounting for flexibility of tank walls on the fluid-structure interaction, Ghaemmaghami and Kianoush [18] studied response of liquid storage tanks. They concluded that the wall flexibility increases the contribution of convective mass, while the contribution of impulsive one remains essentially the same.

The dynamic interaction of flexible container and sloshing liquid was used by Anderson [19] and Gradinscak [20] to control the liquid sloshing. The study was performed using finite element method and confirmed experimentally.

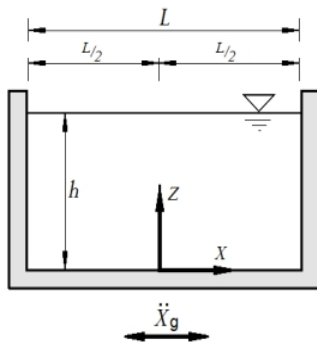


Figure 1. Rigid rectangular liquid storage tank.

This paper investigates the efficiency of a new technique, padded walls, in reducing seismic demand on tank walls. The introduced padded wall changes stiffness and damping characteristics of tank to reduce seismic demand on tank wall. In the following, first the response of tank with rigid wall is derived and then the response of tank with padded wall is obtained. Finally, the effect of pads on seismic response of rectangular tanks are evaluated.

2. RESPONSE OF RIGID TANK

An analytical solution based on velocity potential function is used to derive the response of tank with rigid walls.

Figure 1 depicts the two-dimensional scheme of rectangular tank of partially filled to a height h , subjected to horizontal ground motion excitation. The fluid is supposed to be incompressible and inviscid.

The velocity potential function should satisfy the Laplace equation. In cartesian coordinates, this means:

$$\nabla^2 \varphi = \frac{\partial^2 \varphi}{\partial x^2} + \frac{\partial^2 \varphi}{\partial z^2} = 0 \tag{1}$$

where the boundary conditions of the tank subjected to the ground motion are described as:

$$\left. \frac{\partial \varphi}{\partial z} \right|_{z=0} = 0 \tag{2a}$$

$$\left. \frac{\partial \varphi}{\partial x} \right|_{x=-l/2, l/2} = \dot{X}_g \tag{2b}$$

$$\left. \frac{\partial^2 \varphi}{\partial t^2} + g \frac{\partial \varphi}{\partial z} \right|_{z=h} = 0 \tag{2c}$$

The first boundary condition satisfies the impermeability of the tank on the bottom surface, while the second one describes the lateral motion of rigid walls and the third equation is the free surface boundary condition at $z=h$. Using the method of separation of variables, and satisfying the first and second boundary conditions, the velocity potential function could be derived as:

$$\varphi = x \dot{X}_g + \sum_{n=1}^{\infty} A_n(t) \cosh(\lambda_n z) \sin(\lambda_n x) \tag{3}$$

where λ_n is given by:

$$\lambda_n = \frac{(2n-1)\pi}{l} \tag{4}$$

The modal amplitude $A_n(t)$ is determined by imposing free surface boundary condition (Equation (2c)) on potential function:

$$\sum_{n=1}^{\infty} [\ddot{A}_n(t) \cosh(\lambda_n h) + g A_n(t) \lambda_n \sinh(\lambda_n h)] \times \sin(\lambda_n x) = -x \ddot{X}_g \tag{5}$$

Employing the orthogonality of trigonometric functions, it is possible to uncouple these differential equations to set of N uncoupled differential ones, by multiplying $\sin(\lambda_m x)$ on both sides of Equation (5) and integrating from 0 to $l/2$ which leads to:

$$\ddot{A}_m(t) + \Omega_m^2 A_m(t) = -\mu_m \ddot{X}_g \tag{6}$$

where:

$$\Omega_m^2 = g \lambda_m \tanh(\lambda_m h) \tag{7}$$

$$\mu_m = \frac{4 \int_0^{l/2} x \sin(\lambda_m x) dx}{l \cosh(\lambda_m h)} \tag{8}$$

In the presence of fluid damping, Equation (6) leads to Equation (9):

$$\ddot{A}_m(t) + 2\xi_m \Omega_m \dot{A}_m(t) + \Omega_m^2 A_m(t) = -\mu_m \ddot{X}_g \tag{9}$$

where ξ_m denotes the damping ratio in the n^{th} mode. Solving Equation (9), it is possible to obtain the time evolution of the modal amplitudes. Initially, the tank is considered stationary, and the solutions for this case are conventionally called the ‘‘Eigen functions’’ of the problem.

3. RESPONSE OF TANK WITH PADDED WALL

The aim of employing pads is to change kinematic boundary condition with no control on pressure to kinetic boundary condition. Figure 2 shows the schematic view of pads placed on the walls of the tank.

These pads include numbers of pressurized air packets kept in their positions. The obstruction of airflow in orifices between packets and compressibility of air inside elastic packets establishes damping and stiffness of pads. To simplify the physical treatment of the proposed system, it is modeled as a linear stiffness and damping model. While the governing equations in domain remain the same, the boundary conditions take the following form:

$$\left. \frac{\partial \phi}{\partial z} \right|_{z=0} = 0 \tag{10a}$$

$$\rho \left. \frac{\partial^2 \phi}{\partial t^2} \right|_{x=-l/2} = k \left(\left. \frac{\partial \phi}{\partial x} \right|_{x=-l/2} - \dot{X}_g \right) + c \left(\left. \frac{\partial^2 \phi}{\partial x \partial t} \right|_{x=-l/2} - \dot{\dot{X}}_g \right) \tag{10b}$$

$$\left. \frac{\partial^2 \phi}{\partial t^2} + g \frac{\partial \phi}{\partial z} \right|_{z=h} = 0 \tag{10c}$$

where c and k denote damping and stiffness coefficients of padded wall, respectively. It is evident that the first and third boundary conditions remain the same as the

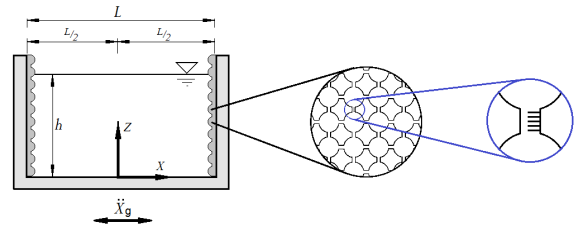


Figure 2. Schematic view of storage tank with padded Walls

rigid ones; while the second one is changed from a kinematic to a kinetic boundary condition. The first boundary condition again denotes the impermeability of the tank bottom surface. The second equation is the equilibrium of force in horizontal direction between pad and fluid and the third equation is again free surface boundary conditions.

To solve the partial differential equations, the potential function should be decomposed to three components as :

$$\phi(x, z, t) = \varphi_1(x, z, t) + \varphi_2(x, z, t) + \varphi_3(x, z, t) \tag{11}$$

Decomposition is done in such a way to have homogenous boundary condition at least for one direction. By this way, we reach to the following boundary conditions for each component:

$$\left. \frac{\partial \varphi_1}{\partial z} \right|_{z=0} = 0 \tag{12a}$$

$$\left. \frac{\partial \varphi_1}{\partial x} \right|_{x=-l/2, l/2} = \dot{X}_g \tag{12b}$$

$$\left. \frac{\partial^2 \varphi_1}{\partial t^2} + g \frac{\partial \varphi_1}{\partial z} \right|_{z=h} = 0 \tag{12c}$$

and

$$\left. \frac{\partial \varphi_2}{\partial z} \right|_{z=0, h} = 0 \tag{13a}$$

$$\left. \frac{\partial \varphi_2}{\partial x} \right|_{x=-l/2} = \frac{\rho}{k} \left(\frac{\partial^2 \varphi_1}{\partial t^2} + \frac{\partial^2 \varphi_2}{\partial t^2} + \frac{\partial^2 \varphi_3}{\partial t^2} \right) - \frac{c}{k} \left(\frac{\partial^2 \varphi_2}{\partial x \partial t} \right) \tag{13b}$$

$$\left. \frac{\partial \varphi_2}{\partial x} \right|_{x=l/2} = -\frac{\rho}{k} \left(\frac{\partial^2 \varphi_1}{\partial t^2} + \frac{\partial^2 \varphi_2}{\partial t^2} + \frac{\partial^2 \varphi_3}{\partial t^2} \right) - \frac{c}{k} \left(\frac{\partial^2 \varphi_2}{\partial x \partial t} \right) \tag{13c}$$

and

$$\left. \frac{\partial \varphi_3}{\partial z} \right|_{z=0} = 0 \tag{14a}$$

$$\left. \frac{\partial \varphi_3}{\partial x} \right|_{x=\pm l/2} = 0 \tag{14b}$$

$$g \frac{\partial \varphi_3}{\partial z} + \frac{\partial^2 \varphi_3}{\partial t^2} \Big|_{z=h} = - \frac{\partial^2 \varphi_2}{\partial t^2} \Big|_{z=h} \tag{14c}$$

It is obvious that the sum of φ_1 , φ_2 and φ_3 satisfies the boundary conditions of Equation (10). The boundary conditions of Equation (12) for φ_1 are exactly the same as the boundary conditions for φ in Equation (2). Therefore, the solution for φ_1 and φ will be the same. This means that sum of φ_2 and φ_3 simulates the difference in the wall pressure between the case of rigid tanks and tanks with padded walls. As k and c increase, φ_2 and φ_3 tend to zero, i.e. the solution becomes closer to the solution of the rigid tank. As a result, the analytical solution of φ_2 and φ_3 are derived by imposing the first and second boundary conditions:

$$\varphi_2 = xB_0(t) + \sum_{n=1}^{\infty} B_n(t) \sinh(\beta_n x) \cos(\beta_n z) \tag{15}$$

$$\varphi_3 = \sum_{n=1}^{\infty} C_n(t) \cosh(\lambda_n z) \sin(\lambda_n x) \tag{16}$$

where β_n is the roots of φ_2 , which is equal to $n\pi/h$.

The time evolution of $B_0(t)$ and modal amplitudes $B_n(t)$ and $C_n(t)$ are determined by imposing the remaining boundary conditions, which means:

$$\ddot{B}_0(t) + \frac{2k}{I\rho} B_0(t) + \frac{2c}{I\rho} \dot{B}_0(t) + \sum_{n=1}^{\infty} \theta_n \ddot{C}_n(t) = -\ddot{X}_g - \sum_{n=1}^{\infty} \theta_n \ddot{A}_n(t) \tag{17}$$

$$\ddot{B}_j(t) + \omega_{2j}^2 B_j(t) + \zeta_j \dot{B}_j(t) + \sum_{n=1}^{\infty} \delta_{jn} \ddot{C}_n(t) = -\sum_{n=1}^{\infty} \delta_{jn} \ddot{A}_n(t) \tag{18}$$

$$\ddot{C}_j(t) + \omega_{1j}^2 C_j(t) + \sigma_j \dot{B}_0(t) + \sum_{n=1}^{\infty} \psi_{jn} \ddot{B}_n(t) = 0 \tag{19}$$

$$\theta_n = \frac{2 \sin(\lambda_n \frac{I}{2})}{Ih} \int_0^h \cosh(\lambda_n z) dz \tag{20a}$$

$$\omega_{2j}^2 = \frac{k\beta_j}{\rho} \times \frac{\cosh(\beta_j \frac{I}{2})}{\sinh(\beta_j \frac{I}{2})} \tag{20b}$$

$$\zeta_j^2 = \frac{c\beta_j}{\rho} \times \frac{\cosh(\beta_j \frac{I}{2})}{\sinh(\beta_j \frac{I}{2})} \tag{20c}$$

$$\delta_{jn} = \frac{2 \sin(\lambda_n \frac{I}{2})}{h \sinh(\beta_j \frac{I}{2})} \int_0^h \cosh(\lambda_n z) \cos(\beta_j z) dz \tag{20d}$$

$$\omega_{1j}^2 = g\lambda_j \tanh(\lambda_j h) \tag{20e}$$

$$\sigma_j = \frac{2}{I \cosh(\lambda_j h)} \int_{-I/2}^{I/2} x \sin(\lambda_j x) dx \tag{20f}$$

$$\psi_{jn} = \frac{2 \cos(\beta_n h)}{I \cosh(\lambda_j h)} \int_{-I/2}^{I/2} \sinh(\beta_n x) \sin(\lambda_j x) dx \tag{20g}$$

Employing the Runge-Kutta method for solution of ODE set of Equations (17-19), the time history of response for $B_0(t)$, $B_n(t)$ and $C_n(t)$ could be derived. Finally, the velocity potential function φ could be evaluated as:

$$\phi = x\dot{X}_g + \sum_{n=1}^{\infty} A_n(t) \cosh(\lambda_n z) \sin(\lambda_n x) + xB_0(t) + \sum_{n=1}^{\infty} B_n(t) \sinh(\beta_n x) \cos(\beta_n z) + \sum_{n=1}^{\infty} C_n(t) \cosh(\lambda_n z) \sin(\lambda_n x) \tag{21}$$

As could be inferred from this equation, the first two terms of this decomposition simulate the response of tank with rigid wall, while the third and fourth terms accounts for pads flexibility.

4. GROUND MOTION RECORDS

The ground motions considered in this study include near-source and far-field records of Elcentro, Kobe and Chi Chi records classified as records in accordance with the fault distance of each of the records. The ground motion records also include Tokach-Oki ground motion which is a long period far-field record. Specifications of records are given in Tables 1 and 2. All ground motions are recorded in soil type C in NEHRP classification [21]. Figures 3 and 4 illustrate the time history and Fourier spectrum of the ground motion records. As could be inferred from Figure 3, amplitude of ground acceleration for near-source ground motions is larger than those for far-field records. Figure 5 shows the large difference between pseudo velocity response spectrum of near-source and far-field ground motion records. As it is evident from this figure, the maximum spectral velocity of near-source records is higher than those of far-field records. In the case of tank with rigid wall the seismic demand on tank wall depends on the amplitude of frequency content at first natural period of tank and lower periods. At the same time, the performance of padded wall in reducing seismic demand mainly depends on the amplitude of frequency content at periods higher than first natural period.

5. VERIFICATION OF MATHEMATICAL FORMULATION

The proposed analytical formulation is validated with numerical solution of Choun and Yun [22]. Figure 5 depicts time history of EW component of 1940 El Centro ground motion together with wave elevation of the rigid tank as evaluated by Choun and Yun (Figure 6b). Figure 6c gives the response padded wall system as

pads stiffness tends to infinity. As could be seen there is a good correlation between Figure 6b and 6c, which validates the formulation put forward in section 3.

TABLE 1. Near-source earthquakes specifications

Designation	Earthquake	Date	Magnitude	Distance (km)
EN	Elcentro	1979/10/15	M (6.5)	8.5
KN	Kobe	1995/01/16	M (6.9)	0.6
CHN	Chi-Chi	1999/09/20	M (7.6)	9.06

TABLE 2. Far-field earthquakes specifications

Designation	Earthquake	Date	Magnitude	Distance (km)
EF	Elcentro	1979/10/15	M (6.5)	23.8
KF	Kobe	1995/01/16	M (6.9)	94.2
CHF	Chi-Chi	1999/09/20	M (7.6)	67.9
T	Tokachi-oki	1968/05/16	MS (8.2)	26.0

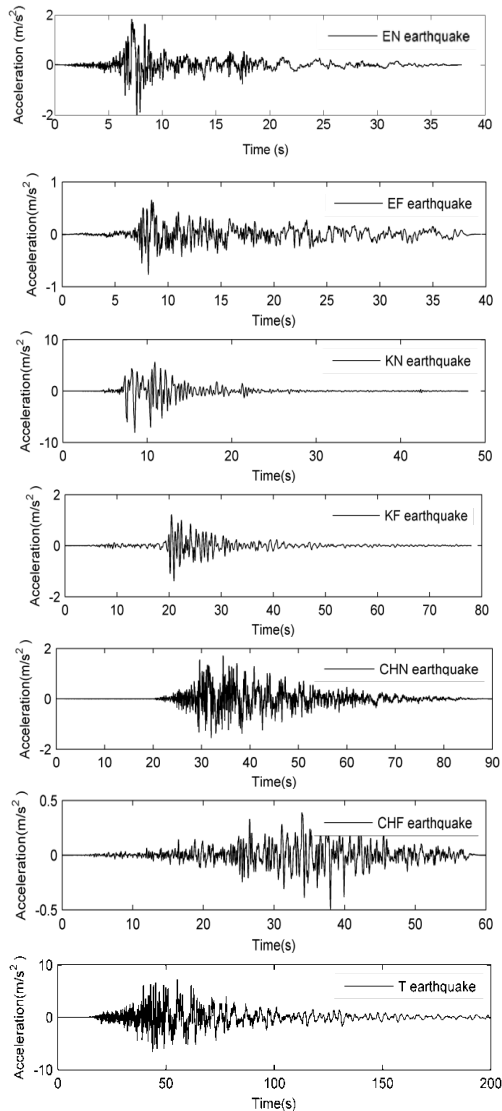


Figure 3. Time history of the input records

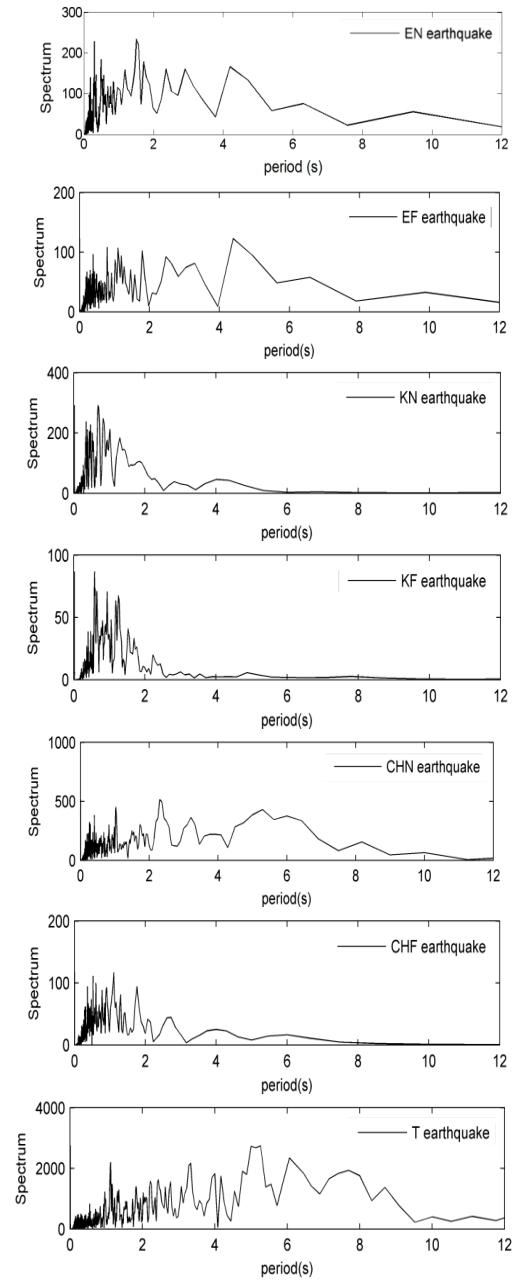


Figure 4. Fourier spectrum of the input records

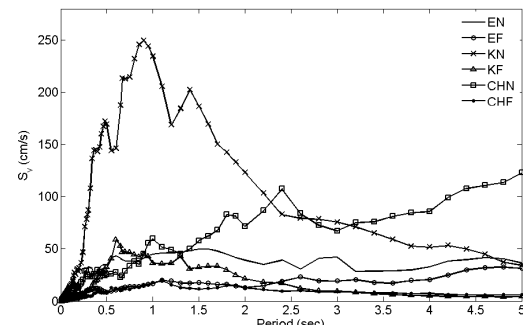


Figure 5. Comparison of pseudo velocity response spectra of studied ground motions for $\xi=0.05$

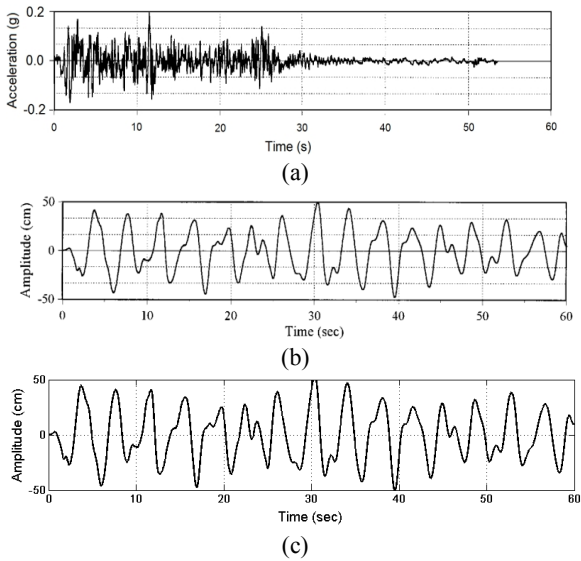


Figure 6. Validation of formulation, a) time history of ground motion, b) wave elevation as evaluated by Chou and Yun [22] and c) wave elevation as evaluated for padded wall with very high stiffness.

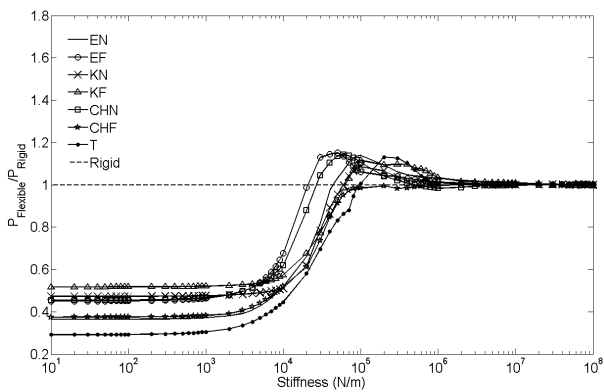


Figure 7. Evolution of the ratio of maximum pressure of the padded wall to the rigid one with pad stiffness for different ground motions.

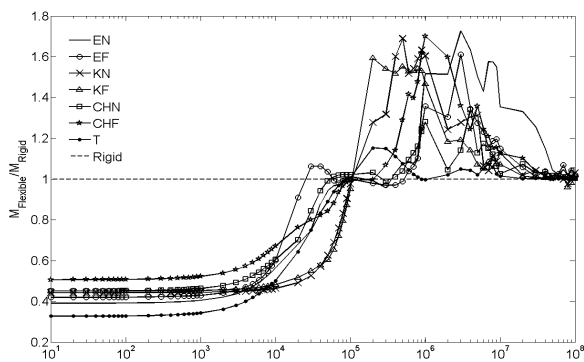


Figure 8. Evolution of the ratio of maximum overturning moment of the padded wall to the rigid one with pad stiffness for different ground motions.

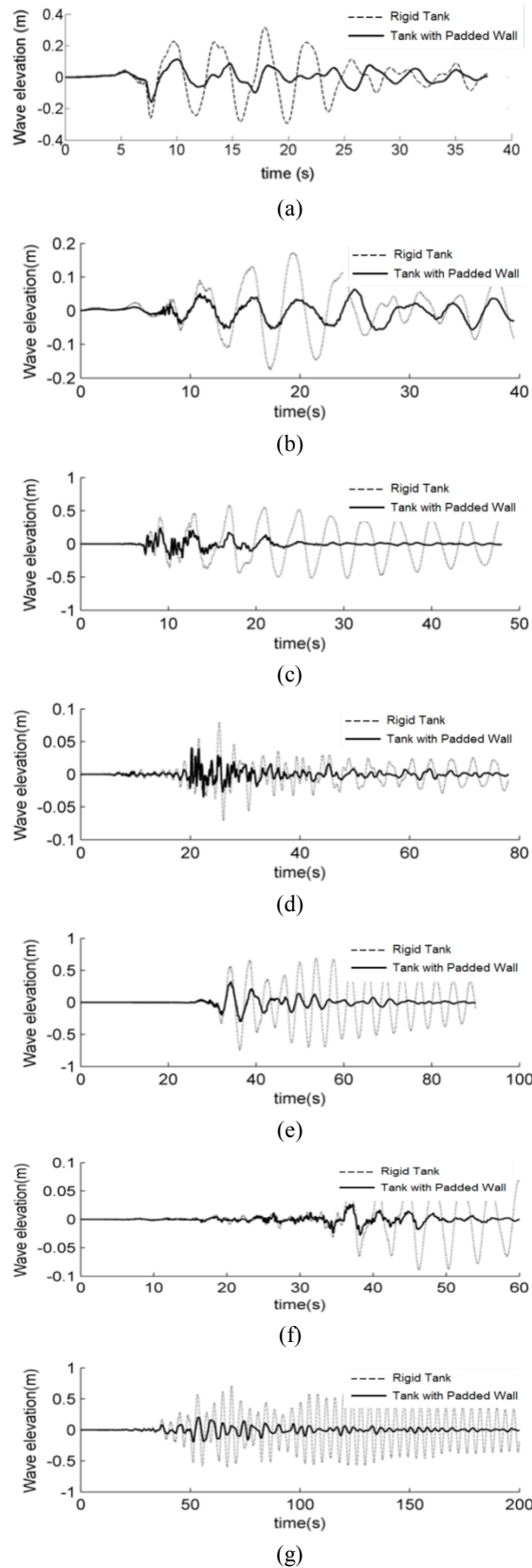


Figure 9. Wave elevation time history for different ground motions, a) EN, b) EF, c) KN, d) KF, e) CHN, f) CHF and g) T.

TABLE 3. Parameters considered for tank in simulations

Tank width	10 m
Liquid height	4 m
Mass density of liquid	1000 kg/m ³
Adopted mode numbers	15
Gravity acceleration	9.81 m/s ²

6. SIMULATION RESULTS

The parameters considered for tank in the simulations are given in Table 3. The first natural period of tank is 3.8 sec. Figure 7 shows the evolution of the ratio of maximum hydrodynamic pressure of the tank with padded wall to the tank with rigid wall. The hydrodynamic pressure is evaluated at water surface. At the same time, Figure 8 depicts the evolution of the ratio of overturning moment of the padded wall to rigid one. Both figures are evaluated for padded wall with damping coefficient of 10 kN.s/m and different values for stiffness of pad. According to Figures 7 and 8, it can be noted that there is about 50% decrease in max pressure and overturning moment in the case of padded wall for pad stiffnesses smaller than 20 kN/m. Also as expected, for large values of pad stiffness the response of tank with padded wall tends to those of rigid one.

Comparing Figures 7 and 8, reveals that different pattern of behavior occurs for different response parameters. While in the case of wave elevation the response for all records tends to the response of rigid tank at pad stiffness of about 1000 kN/m, for overturning moment it only tends to the response of rigid tank at pad stiffness of about 10⁵ kN/m. The main reason for different patterns of response evolution for increasing pad stiffness is that wave elevation is mainly controlled by displacement spectrum of the records, while the overturning moment is mainly controlled by acceleration spectrum.

From Figures 7 and 8, it could be concluded that pad stiffness of 1 kN/m will give optimum value for reduction of sloshing height and force induced on tank wall. Figures 9 and 10 give the response of the tank for this optimum value of pad stiffness (1 kN/m). Figure 9 shows the wave elevation-time history and Figure 10 depicts the distribution of pressure along wall height when hydrodynamic pressure results in maximum shear. These figures compares the response of tank with rigid wall and tank with padded wall for tank subjected to aforementioned ground motion records.

As could be seen there is substantial reduction in wave elevation and maximum water pressure exerted on tank walls. It is also evident that there is no significant differences in the response for near field and far field records and in both cases the system is able to have appreciable impact on the response.

The decrease in the response amplitude is more pronounced for KN, KF, CHN and CHF as these records are only rich in low period component (Figure 5). Use of pads increases the system period where these records have weaker frequency content. This is not the case for EN and EF as these records are also rich in high periods. This results in smaller reduction in response amplitudes for these records.

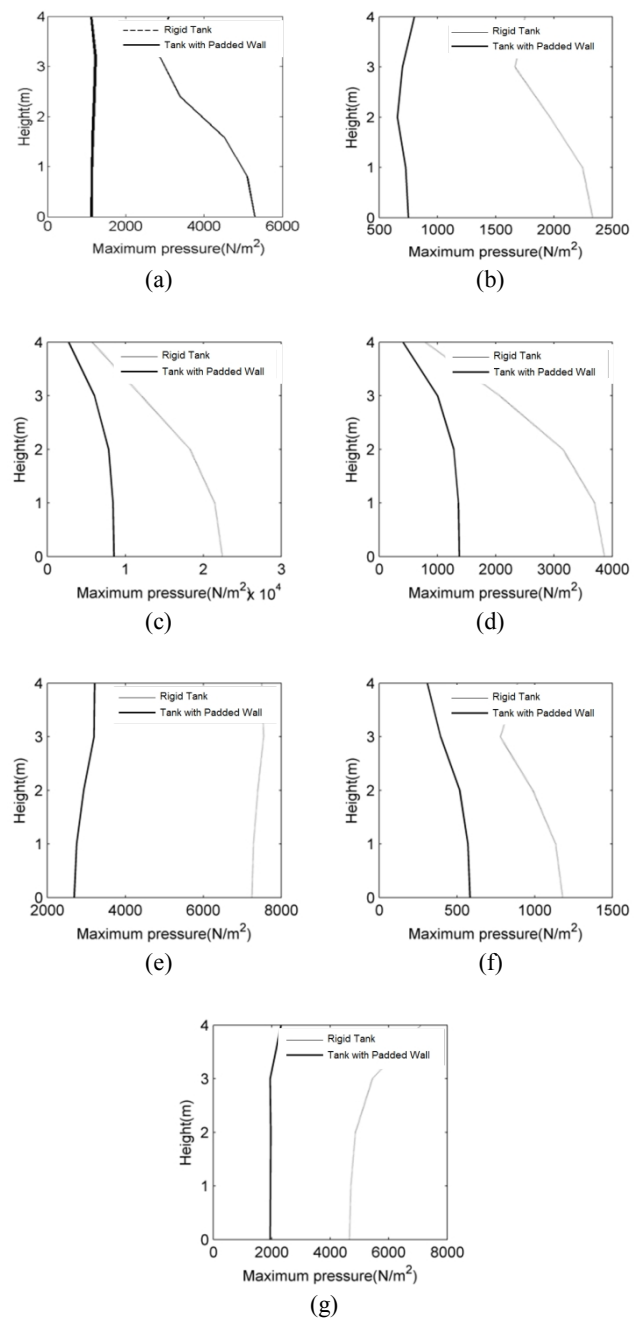


Figure 10. Dynamic pressure distribution on the tank wall, a) EN, b) EF, c) KN, d) KF, e) CHN, f) CHF and g) T.

The main idea of this paper is to change kinematic boundary condition at tank wall to kinematic boundary condition. In usual tanks with rigid wall where boundary condition is kinematic, there is no control on the force (pressure) exerted on the wall. On the other hand, in padded wall the boundary condition becomes kinetic, which makes it possible to control seismic force demand on the tank wall. This paper deals with theoretical aspects of employing this concept in seismic retrofit of tanks, while practical issues related to endurance, health, aging of pads and their chemical properties need to be thoroughly investigated.

7. CONCLUSION

A new method is proposed to reduce seismic demand on tanks wall. An analytical solution based on velocity potential function is proposed to investigate the wave elevation and maximum pressure on the wall of the rigid tank and tank with padded wall. The aim of this study is to estimate optimum padded wall structural property to reduce sloshing response of tank subjected to ground motion records of different types including far-field and near source records. It is concluded that the proposed method could substantially reduce the wave elevation and the pressure on tank wall.

8. REFERENCES

1. Abramson, H.N., "The dynamic behavior of liquids in moving containers. Nasa sp-106", *NASA Special Publication*, Vol. 106, (1966).
2. Hwang, J., Kim, I., Seol, Y., Lee, S. and Chon, Y., "Numerical simulation of liquid sloshing in three-dimensional tanks", *Computers & Structures*, Vol. 44, No. 1, (1992), 339-342.
3. Virella, J.C., Prato, C.A. and Godoy, L.A., "Linear and nonlinear 2d finite element analysis of sloshing modes and pressures in rectangular tanks subject to horizontal harmonic motions", *Journal of Sound and Vibration*, Vol. 312, No. 3, (2008), 442-460.
4. Wang, C. and Khoo, B., "Finite element analysis of two-dimensional nonlinear sloshing problems in random excitations", *Ocean Engineering*, Vol. 32, No. 2, (2005), 107-133.
5. Tariverdilo, S., Shabani, R. and Salarieh, H., "Effect of flexural and membrane stiffnesses on the analysis of floating roofs", *International Journal of Engineering-Transactions A: Basics*, Vol. 23, No. 1, (2009), 57-64.
6. Shabani, R., "Stress patterns in single deck floating roofs subjected to ground motion accelerations", *International Journal of Engineering-Transactions C: Aspects*, Vol. 26, No. 12, (2013), 1495-1504.
7. Azhdari Moghadam, M., "Analysis and design of a simple surge tank", *International Journal of Engineering, Transactions A: Basics*, Vol.17, No.4, (2004), 339-345.
8. Isaacson, M. and Premasiri, S., "Hydrodynamic damping due to baffles in a rectangular tank", *Canadian Journal of Civil Engineering*, Vol. 28, No. 4, (2001), 608-616.
9. Akyıldız, H., Erdem Unal, N. and Aksoy, H., "An experimental investigation of the effects of the ring baffles on liquid sloshing in a rigid cylindrical tank", *Ocean Engineering*, Vol. 59, (2013), 190-197.
10. Cho, J. and Lee, H., "Numerical study on liquid sloshing in baffled tank by nonlinear finite element method", *Computer Methods in Applied Mechanics and Engineering*, Vol. 193, No. 23, (2004), 2581-2598.
11. Panigrahy, P., Saha, U. and Maity, D., "Experimental studies on sloshing behavior due to horizontal movement of liquids in baffled tanks", *Ocean Engineering*, Vol. 36, No. 3, (2009), 213-222.
12. Jung, J., Yoon, H., Lee, C. and Shin, S., "Effect of the vertical baffle height on the liquid sloshing in a three-dimensional rectangular tank", *Ocean Engineering*, Vol. 44, (2012), 79-89.
13. Pal, P. and Bhattacharyya, S., "Sloshing in partially filled liquid containers—numerical and experimental study for 2-d problems", *Journal of Sound and Vibration*, Vol. 329, No. 21, (2010), 4466-4485.
14. Koller, M.G. and Malhotra, P.K., "Seismic evaluation of unanchored cylindrical tanks", in 13th world conference on earthquake engineering, Vancouver, BC, Canada., (2004).
15. Liu, D. and Lin, P., "Three-dimensional liquid sloshing in a tank with baffles", *Ocean Engineering*, Vol. 36, No. 2, (2009), 202-212.
16. Belakroum, R., Kadja, M., Mai, T. and Maalouf, C., "An efficient passive technique for reducing sloshing in rectangular tanks partially filled with liquid", *Mechanics Research Communications*, Vol. 37, No. 3, (2010), 341-346.
17. Maleki, A. and Ziyaeifar, M., "Sloshing damping in cylindrical liquid storage tanks with baffles", *Journal of Sound and Vibration*, Vol. 311, No. 1, (2008), 372-385.
18. Ghaemmaghami, A. and Kianoush, M., "Effect of wall flexibility on dynamic response of concrete rectangular liquid storage tanks under horizontal and vertical ground motions", *Journal of Structural Engineering*, Vol. 136, No. 4, (2009), 441-451.
19. Anderson, J.G., "Liquid sloshing in containers: Its utilisation and control", Victoria University of Technology, (2000).
20. Gradinscak, M., Semercigil, S. and Turan, O., A sloshing absorber with a flexible container, in Structural dynamics, Vol. 3, (2011), Springer, 315-322.
21. B.S.S.C., "Nehrp recommended provisions for seismic regulations for new buildings and other structures, FEMA 450, developed by BSSC for FEMA Washington, (2003).
22. Choun, Y.S. and Yun, C.B., "Sloshing analysis of rectangular tanks with a submerged structure by using small-amplitude water wave theory", *Earthquake Engineering & Structural Dynamics*, Vol. 28, No. 7, (1999), 763-783.

Introducing Padded Wall to Reduce Sloshing Induced Wall Pressure in Water Storage Tanks

R. Mahmoudi, F. Ashrafzadeh, S. Tariverdilo

Department of Civil Engineering, University of Urmia, Urmia, Iran

PAPER INFO

چکیده

Paper history:

Received 13 February 2014

Received in revised form 01 August 2014

Accepted 14 August 2014

Keywords:

Sloshing

Velocity Potential Function

Padded Wall

Water Storage Tank

در هنگام وقوع زلزله سیال درون مخازن ذخیره سیالات دچار موج شدگی شده که منجر به اعمال فشار دینامیکی مضاعف بر دیواره مخزن می شود. مطالعه حاضر به بررسی تاثیر بالشتک هوا بر روی پاسخ مخازن آب مستطیلی تحت تحریک زلزله می پردازد. روش حل به صورت تحلیلی و بر اساس تابع پتانسیل سرعت می باشد که به منظور استخراج پاسخ مخازن به صورت ارتفاع موج، فشار ماکزیمم در دیواره مخزن و طیف تبدیل فوریه فشار در سطح آب مخازن صلب با و بدون بالشتک هوا در دیواره مخزن ارائه شده است. در روش ارائه شده علاوه بر شرایط مرزی سینماتیکی متداول در روشهای معمول، شرایط مرزی سینماتیکی نیز به صورت توزیع فشار بر روی دیواره مخزن اعمال شده است. سیال داخل مخزن به صورت غیر ویسکوز و تراکم ناپذیر و جریان غیرچرخشی فرض شده است. رفتار لرزه ای مخازن مورد نظر تحت تحریک زلزله های متفاوت در حوزه دور و نزدیک مورد بررسی قرار گرفته اند. نتایج نشانگر عملکرد بهینه بالشتک هوا در کاهش فشار و ارتفاع موج سیال می باشد.

doi: 10.5829/idosi.ije.2014.27.12c.04
